

The influence of material colors on the *effective color rendering and temperature* through mutual illumination

Cehao Yu, MSc, MCIBSE, MSL, CEng¹ and Prof. dr. Sylvia Pont¹, 1: *Perceptual Intelligence lab (π-lab), Faculty of Industrial Design Engineering, Delft University of Technology, Delft, The Netherlands*

Abstract

In complex scenes, the light reflected by surfaces causes secondary illumination, which contributes significantly to the actual light in the space (the "light field"). Secondary illumination is dependent on the primary illumination, geometry, and materials of a space. Hence, primary illumination and secondary illumination can have non-identical spectral properties, and render object colors differently. Lighting technology and research predominantly relies on the color rendering properties of the illuminant. Little attention has been given to the impact of secondary illumination on the "effective color rendering" within light fields. Here we measure the primary and secondary illumination for a simple spatial geometry and demonstrate empirically their differential "effective color rendering" properties. We found that color distortions due to secondary illumination from chromatic furnishing materials led to systematic and significant color shifts, and major differences between the lamp-specified color rendition and temperature and the actual light-based "effective color rendering" and "effective color temperature". On the basis of these results we propose a methodological switch from assessing the color rendering and temperature of illuminants only to assessing the "effective color rendering and temperature" in context too.

Keywords

Effective color rendering, Effective color temperature, Secondary illumination, Light fields, Material-light interactions

Introduction

In the natural world, the effective illumination or light field, is usually composed of primary illumination emanating directly from a light source, and secondary illumination reflected by objects (f.i. the floor, walls and ceiling of a room). The chromatic properties of the secondary illumination are a product of the primary lighting's spectral power distribution and the object material's spectral reflectance function. Therefore, the spectral shapes of primary illumination and secondary illumination are often different, unless the secondary illumination is originating in achromatic surfaces.

The perceived color of light scattered from objects is termed object color. Visual mechanisms such as chromatic adaptation and color constancy have a major impact on perceived object colors (the "output"). Here we will, however, ignore such effects and firstly focus on the *input* to the human visual system, that is, the optical effects of material colors. Object color varies as a function of illumination spectral power distribution and material spectral reflectance. Despite the material spectral reflectance function being inherent, object color is thus subject to the chromatic properties of both primary and secondary illumination. Color rendition measures (CRMs) are extensively used in lighting

design. They apply to lamps and characterize their effects on the color appearances of a representative set of colored surfaces, relative to an ideal or natural light source. Daylight or a full spectrum radiator such as incandescent light are generally used as a reference, since the color appearances of objects revealed by such illumination appear to be natural for normal color vision and full spectra contain power at all visible wavelengths, facilitating color rendition. CRMs quantify how well object color appearances are reproduced or revealed by a specified illumination in comparison with metameric full spectrum radiators. With complete immersion in and adaptation to the chromaticity of the specified illumination, CRMs assume the best possible constancy with respect to the reference illumination. Illumination with good color rendering, in general, makes object colors look to be similar to observers' expectations. Deviations of apparent colors from those under the reference illumination cause poor color rendering.

There are multiple CRMs in use to quantify the color rendering performance, among which the CIE color rendering index (CRI) R_a , which is the most widely used measure. Despite its prominence, it has a variety of limitations [1], [2]. Concerns include inaccurate calculations due to inadequate (15 in total) test color samples (TCS), the use of sub-optimal color coordinates, outdated chromatic adaptation calculation and a harsh cutoff at 5000 K for defining the reference illuminant. The index being a scalar or single average value also falls short of indicating the type of color effect, i.e. whether it concerns a (de)saturation effect or a hue shift. As a pure fidelity metric based on an absolute scale, the relative color desirability or color preference is not assessed. There has been continuous interest in examining the validity and utility of new metrics as a replacement [3]–[8] or an adjunct [9] to the CRI. Global consensus was reached on assessing color rendering via TM-30 [10], [11]. TM-30 specifies both an improved fidelity index (R_f) and a gamut index (R_g), accompanied by a color distortion graphic. Its increased number (99 in total) of color evaluation samples (CES) covers a wide range of reflectance spectra, corresponding to a range of consumer goods and natural objects. Instead of a sharp cutoff at 5000 K, TM-30 uses a blended model between 4500 K and 5500 K for a continuous referent illuminant. The additional R_g and color distortion graphic provide detailed information on the hue and saturation shifts. However, a switch to TM-30 in practice involves both hardware and software upgrading and therefore time, so characterizing color rendition by the CRI is still in use. The current study will therefore use both the more conventional and the more state-of-the-art color fidelity measures to characterize the effects of secondary illumination on color rendition, which we coin the "effective color rendering".

Lighting technology and research generally relies on the color rendering of primary illumination. The impact of secondary illumination on the "effective color rendering" is usually not taken into account. To overlook this however can lead to unacceptable color distortion in practical applications [3], [12]. In Figure 1, bottom row, a light gray matte test surface patch is located in the

center of two identical windowless box rooms (with the length, width and height to be 6000mm x 3300mm x 3300mm). One room is furnished matte white and the other orange. Both material colors have the same brightness value. The primary illumination of both box rooms is the same neutral white luminous panel (1884mm x 773mm). Despite the good color rendering of the primary illumination, the apparent colors of the test surface patches are rather different, namely gray versus orangish. Owing to the identical geometrical configuration and lighting distribution, the color rendering of the test surface patch in the primary illumination images (the images in the top row) is the same for both conditions - and this is exactly what conventional CRMs represent. The middle row shows the contribution of the indirect or secondary illumination on the color rendering of the test patches. Current practice assumes that secondary illumination is achromatic or has minimal impact on color rendering - as in the left column of Figure 1. The orange room of the right column presents a quite extreme example, however, it does demonstrate that the impact of context on color rendering cannot be ignored and that the "effective color rendering" including such contextual effects deserves attention.

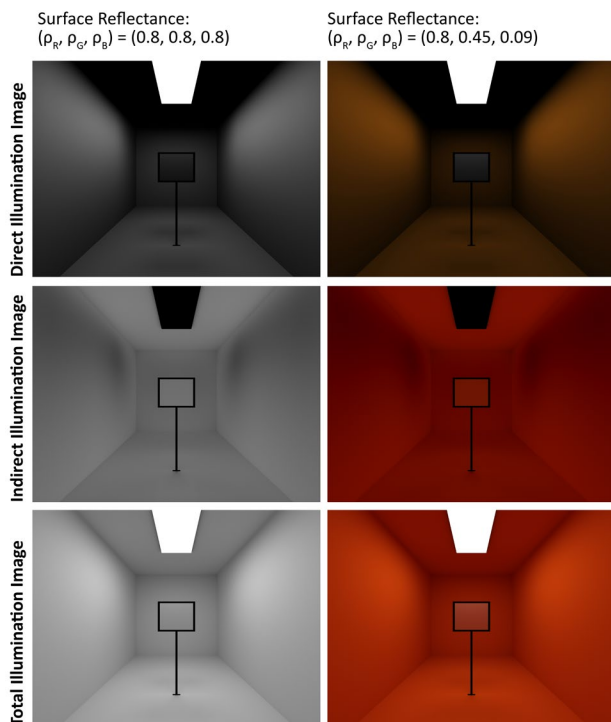


Figure 1. Simulation of an achromatic patch in a box room furnished in matte white (left) and orange (right) illuminated by an identical neutral white direct light source. Direct, indirect and total illumination renders (in the rows) illustrate the contributions from primary and secondary illumination and the final result.

Moreover, Bloj et al [13] showed that for Mach cards human observers could only partially compensate for secondary illumination when viewing the folded cards with normal binocular disparities. The study featured only one spatial configuration and color combination. Doerschner et al [14] considered a series of spatial configurations for one color combination. It was found that human observers discounted inter-reflections more when it was more intense and that they tended to under-compensate for the secondary illumination. Thus, the empirical proof shows that

human observers are sensitive to local chromatic effects of inter-reflections but can only partially discount its impact in natural scenes. Here we focus on characterizing and quantifying these spatial effects on CRMs.

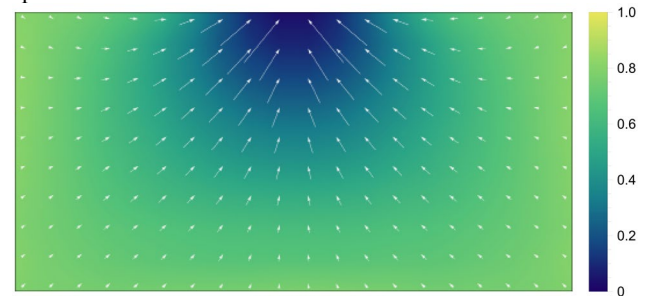


Figure 2. Schematic presentation of the first order light field properties in a room with a single source in the center. The light vectors are represented by arrows and show the "light flow", diverging out from the source to the light absorbing surfaces. The false color map indicates the level of diffuseness, ranging from 0 (collimated light) to 1 (spherically diffuse).

In order to measure, describe, and visualize spatially varying lighting distributions, the current study makes use of the 'Delft light field framework' [15]. The physical light field (the spectral power as a function of position, direction and wavelength) represents the luminous environment completely. It can be decomposed as the sum of qualitatively different components, i.e. ambient, focus and brilliance light. The ambient light corresponds to fully diffuse illumination or uniformly distributed spectral energy. It can be represented by a scalar and physically corresponds to the light density. Focus light concerns directed lighting with one main (average) direction. It can be represented by a vector and physically corresponds with the net flux transport. Brilliance light, represented by luminous patterns or light textures, refers to its angular and spatial high frequencies. Real-world light can be described as a weighted linear sum of those components, as a function of position. Next to capturing light fields and comparing them to their perceptions (the "visual light fields" [16]) this framework is used to design light(ing), synthesizing the optical, perceptual and design knowledge in a simple and easy to understand linear combination of just three canonical light modes. Please note that light fields capture the effective light in a space, the result of primary *and* secondary illumination, including (inter)reflections, shad(ow)ing effects, etcetera, so it describes the actual complex lighting distribution that is potentially available to the human visual system (or "plenoptic function" [17]). The light field thus depends on the light source characteristics, the space's geometry, the materials and, if present, the objects in the space. In past studies the first order characteristics of light fields were described, measured and visualized or, in other words, spatial variations of light density, direction and diffuseness throughout architectural spaces (15, 21, 22), see Figure 2.

The aim of this study is to extend this with predictions and measurements of the chromatic variations within those light fields and their impact on the resulting color rendering. The current paper introduces the concept "effective color rendering" to capture this impact and demonstrates the main phenomena, as a first step to quantify the complexity of the underlying optical mechanisms.

Chromatic effects of secondary illumination

Consider the uni-chromatic space in Figure 1. The spectral power distribution of the direct light source is denoted as $E_0(\lambda)$,

the surface reflectance function of the room as $\rho_R(\lambda)$. The effective illumination at any point of the space is a weighted sum of primary illumination $E_P(\lambda)$ and secondary illumination $E_S(\lambda)$ (Figure 3), where

$$E_P(\lambda) = \gamma_0 E_0(\lambda) \quad (1)$$

$$E_S(\lambda) = \sum_{i=1}^{\infty} \gamma_i E_0(\lambda) \rho_R(\lambda)^i \quad (2)$$

The weighting (*geometric factors*) γ_i are determined by the spatial geometry, the illuminant's lighting distribution and the material's BRDF (bidirectional reflectance distribution function). If the room surface is achromatic (a flat spectral reflectance function), then each reflection has the same spectrum shape. For a colored room, the spectrum shape changes with each reflection. The i -th bounce reflection results in a multiplier of the i -th power of the material spectral reflectance function to $E_0(\lambda)$. As a result, the spectrum shape of the secondary illumination depends strongly on $\rho_R(\lambda)$.

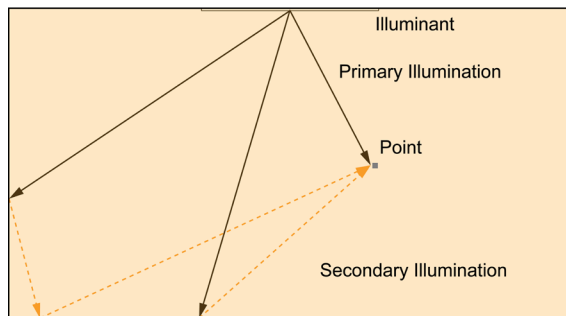


Figure 3. Illustration of effective illumination, as a combination of primary and secondary illumination, at any point of the box room.

Since the absolute spectral power attenuates exponentially (Equation 2), the relative differences between the peak(s) and trough(s) of the material spectral reflectance increase with each bounce. The color of the secondary illumination thus shifts towards the spectral peak of the material reflectance. We [18] found different types of chromatic effects due to inter-reflections, resulting in brightness, saturation and hue variations. That also explains why the indirect illumination image of the orange room (of which the spectral reflectance peak is in the long wavelength range) in Figure 1 is reddish.

Due to chromatic effects of secondary illumination, the objects are, in effect, rendered differently than with primary illumination only. The color differences of test color samples revealed under a direct light source and under a reference illuminant quantify the color rendering of the primary illumination. For a colored room with the same illuminant, the secondary illumination will cause variations of color fidelity.

Empirical testing 1: Color rendering variations in a physical box space

Chromatic effects of inter-reflections have a major influence on the ambient light field component due to its diffuse nature, and a minor influence on the focus light [18]. The "effective color rendering" properties of the actual light in a space are therefore predicted to vary as a function of the contribution of the ambient and focus light field components: the more primary lighting (often consisting of a major focus and minor ambient contribution), the more it will be consistent with the original color rendering measures, and the more secondary lighting (a major ambient and

minor focus contribution, f.i. in the back corners of our room), the more the color rendering will deviate. Here we empirically test how chromatic effects of secondary illumination affect the color rendering for different components of the "Delft light field framework".

Methods

A series of mock up box rooms were constructed like those in Figure 1. The spaces were furnished in four different material colors, i.e. white, maroon, coral and orange, representing cases in which the secondary illumination shows brightness, saturation and hue shifts. The box rooms were illuminated by a xenon lamp via a diffusing panel. In Figure 4, the spectral power distribution, color rendering index (CRI) and TM-30 measurements of the primary illumination are represented.

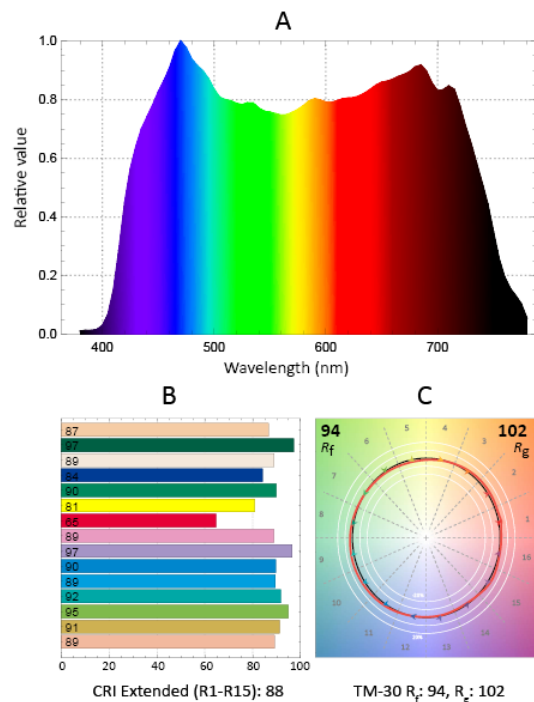


Figure 4. A. Spectral power distribution of the primary illumination. B. Bar plots of the Color Rendering Index (R_i) values for all 15 CIE test color samples and the calculated CRI extended R_a (R_1-R_{15}). C. TM-30 color fidelity index (R_f), gamut index (R_g) and color distortion graphic.

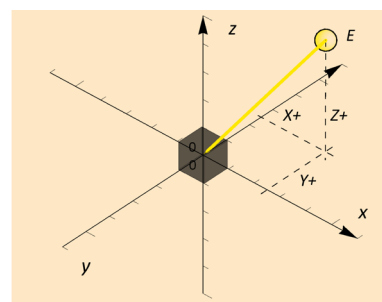


Figure 5. The frame of reference for the cubic illumination measurements.

The effective color rendering in the corners is predicted to deviate more from the color rendering of the light source than the color rendering in the center, due to chromatic effects of inter-reflections. The local light fields in the center and corner were

measured via spectral cubic illuminance (Figure 5) [15], [19]–[22]. Using Cartesian coordinates, E_{x+} and E_{x-} represent the spectral illuminance measurements in the positive and negative directions along the X axis, and analogous for the Y and Z directions. The ambient light is estimated via the mean incident spectral illuminance of the six cubic faces (Equation 3). The square root average of differences in the three orthogonal directions gives an estimate of the focus light (Equation 4). These calculations were done as a function of wavelength (not shown in the equations for simplicity).

$$E_a = \frac{E_{x+} + E_{x-} + E_{y+} + E_{y-} + E_{z+} + E_{z-}}{6} \quad (3)$$

$$E_f = \sqrt{(E_{x+} - E_{x-})^2 + (E_{y+} - E_{y-})^2 + (E_{z+} - E_{z-})^2} \quad (4)$$

The spectral power distributions of the ambient and focus light vary due to different contributions of the primary and secondary illumination, and are expected to show a different effective CCT and CRI.

Results

Figure 6 shows the effective CCT (left graphs) and CRI (right graphs) of the ambient (yellow bars) and focus (blue bars) components in both the center (top row) and the corner (bottom row) of the box rooms, which were calculated based on the spectral power distribution of the actual ambient and focus light in the room. The values for the white room are similar to the values for the illuminant (represented by the dashed reference line). For the other three finishes, the effective CCTs and CRIs of the ambient illumination are lower than for the focus light. The effective CCT and CRI of the ambient light differed up to about 2000K and 50% from the reference illuminant values that the lighting industry relies on in practice. The effective CCT and CRI of the focus light were more consistent with the reference illuminant value, but still deviated up to 700K and 10% in the corner.

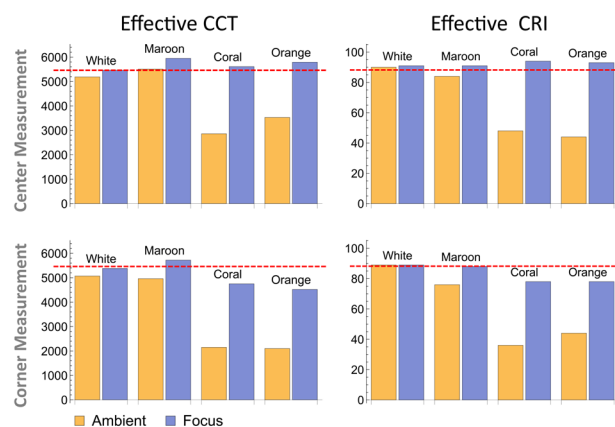


Figure 6. Effective CCT (left) and CRI (right) measurements for ambient and focus components (yellow and blue bars) measured in the center (top row) and corner (bottom row).

Figure 7 shows the effective TM-30 measurements for the ambient (the first and third columns) and focus (the second and fourth columns) components of the four colored rooms in the

center (the first and third rows) and corner (the second and fourth rows). The pattern of the results was consistent with that of the effective CRI measurements. The color rendition for the two light field components was almost identical in the white room, but mutually different in the colored rooms. The effective color fidelity of the ambient light components decreased up to 25% compared to that of the light source and showing both saturation increases and hue shifts. The deviations in the corner were found to be larger than in the center. Also, they were found to be larger for material colors with a high albedo and brightness value (coral and orange) than for a low albedo and brightness value (maroon).

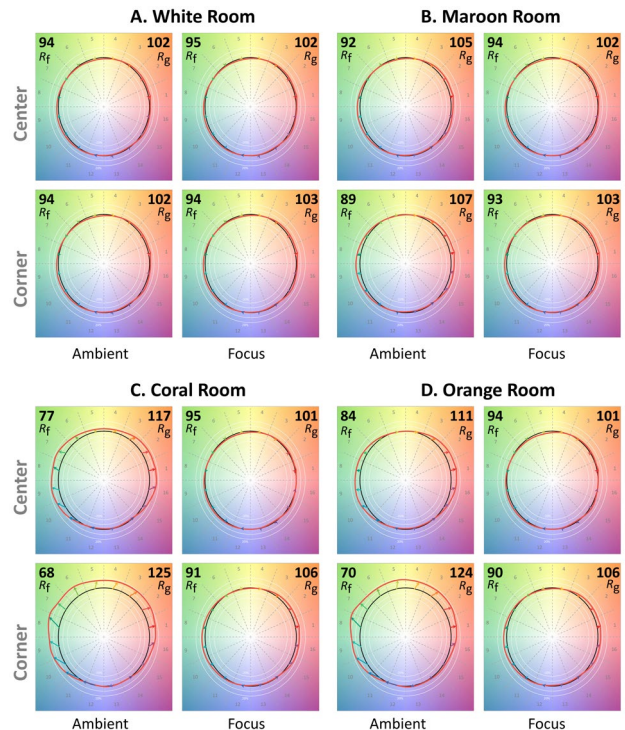


Figure 7. Effective TM-30 measurements for the ambient (the first and third columns) and focus (the second and fourth columns) components of A. white, B. maroon, C. coral and D. orange room in the center (the first and third rows) and corner (the second and fourth rows).

Intermediate discussion

Material colors of a space can alter the illuminant's color rendering in that space due to inter-reflections. Major impacts were found in the quite extreme cases of uniformly colored coral and orange boxes, which colors have high albedo and brightness values. The white reference room showed only minor effects, which were probably due to the white paint not being perfectly "white". For the maroon box, having a color with low albedo and brightness values, the absolute spectral power of the secondary illumination is weak with respect to primary illumination. It thus demonstrated relatively small effects on the effective CCT, CRI and TM-30 measures.

Empirical testing 2: Color rendering variations in computer simulations of a box space

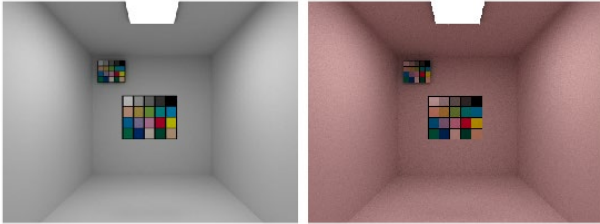
To quantify the effects for more representative material finishes and visualize their impact on color appearances in a space, we simulated a wide range of material finish colors via

computer renderings, for the box space and neutral white primary illumination.

Illuminant Spectrum:
 $(E_R, E_G, E_B) = (0.8, 0.8, 0.8)$

Surface Reflectance:
 $(\rho_R, \rho_G, \rho_B) = (0.8, 0.8, 0.8)$

Surface Reflectance:
 $(\rho_R, \rho_G, \rho_B) = (0.8, 0.75, 0.75)$



Surface Reflectance:
 $(\rho_R, \rho_G, \rho_B) = (0.75, 0.8, 0.75)$

Surface Reflectance:
 $(\rho_R, \rho_G, \rho_B) = (0.75, 0.75, 0.8)$

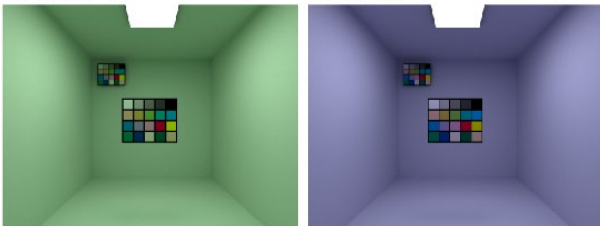


Figure 8. A collection of linearly tone mapped HDR rendered images of box rooms with customized color checkers placed in the center and upper-left corner.

Methods

In order to measure the effective color rendering for a large sampling of colors we simulated a CRI color checker in a box room. The color checker was made of the 15 CIE test color samples and 5 achromatic color samples. We placed two color checkers in the center and upper left corner of the box room. In the corner the contribution of secondary illumination was stronger. The color of the illuminant is neutral white, with 5500K CCT and 100 CRI. Four different colors were allocated to the room surfaces (Figure 8), namely neutral white and low saturated primary colors with the same brightness value. The neutrally colored white room is a control condition, since the spectral shape of the inter-reflected light is constant and the same as the illuminant. The effective color rendition in the white room is thus equal to the original value for the illuminant. The selected finish colors have spectral peaks in one RGB channel and troughs for the other two channels. Colors of low saturation are more realistic in the sense of more frequent applications in architecture.

Results

The described four conditions were simulated and the HDR output images were linearized. The collection of color checkers from the center and corner of each room were cropped from the linearly tone mapped images (Figure 9). The left column shows the color checkers placed in the center and corner of the white room, as reference conditions. Those of the colored rooms were grouped in the three right columns. For comparison, the brightness values of the color checkers in the center and corner were equalized based on their achromatic scales.

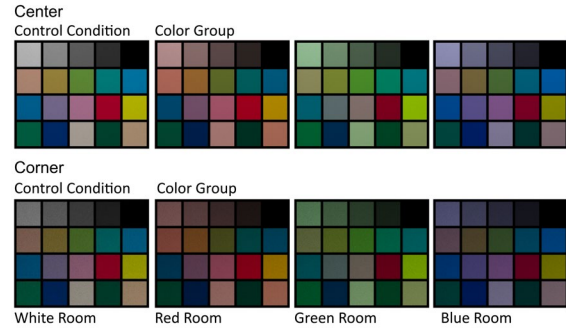


Figure 9. Apparent color appearance of a customized color checker in the differently colored box rooms above, in the center and back corner (in the rows). The color checkers from the white room provide the references, to compare those of the color group against.

The spectral power distributions of the effective illumination incident on the color checkers can be estimated by the color appearances of the white samples. The effective CCTs and CRIs of the center and the corner for the four conditions were then calculated on this basis (Figure 10). We found that the effective CCT differed on average 700K in the center and 1000K in the corner, while the effective CRI differed on average 10% (center) and 16% (corner). The red room caused a major decrease of the CCT and the blue room a major increase.

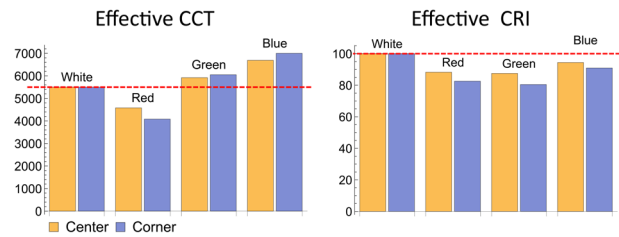


Figure 10. Effective CCT (left) and CRI (right) measurements for illumination incident on the color checkers in the centers and corners (yellow and blue bars) in the four rooms of Figure 6.

Effective TM-30 measurements for the center (upper row) and corner (lower row) of the control condition (left column) and color group (right three columns) are shown in Figure 11. The effective R_f in the color group differed up to 8% with respect to control condition despite the low saturation of the finish material colors. The color fidelity losses in the corners are slightly larger than in the centers.

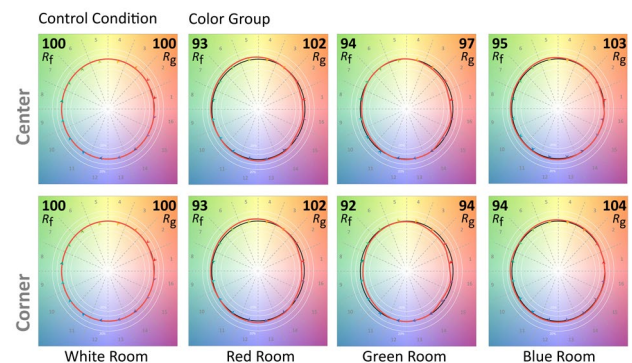


Figure 11. Effective TM-30 measurements for the center (upper row) and corner (lower row) of the control condition (left column) and color group (right three columns).

Discussion

Color rendering is a crucial factor for lighting applications. This study demonstrated that the chromatic properties of furnishing materials are of influence on the *effective color rendering* within a light environment. This effect is due to mutual illumination, which is often ignored in practice, but as shown here can have a major impact on the actual appearance.

The spectral properties of the effective illumination and its color rendering are dependent on scene and object geometry, the spectral power distribution of the illuminant and the material spectral reflectance function. Determining the effective color rendering and CCT is therefore complex. However, it was demonstrated that in some cases the differences between spectrally neutral reference and *effective color rendering and CCT* were extremely large and thus worth considering.

This study was limited to Lambertian materials, simple uniformly colored box spaces and full spectrum lighting. Natural scenes can have complex geometries and contain more diverse materials with more complex reflectance functions. Primary lighting can have all sorts of spectral properties. The main challenge is thus to develop a method to approach this endless range of possibilities in a systematic manner. Next to this challenge of capturing the optical effects, there is the one capturing the visual effects. In the future, we will investigate visual responses to spatially varying light characteristics including color rendition via psychophysical experiments.

In conclusion, the *effective color rendering* in any environment was shown to be strongly dependent on not just the illuminant but also the surrounding material colors. The spectral shape of the indirect light field component is predominantly defined by scene material spectral reflectance, while the illuminant is the crucial determinant for that of the direct component. On the basis of these results we propose to also assess the environment's "effective color rendering and temperature" in applications, in addition to the illuminant's characteristics. Treating the indirect and direct illumination in a linear model allows capturing and understanding the influences of illuminant and scene separately, and analyzing the variation of spectral energy throughout a scene (or light field) in a systematic manner.

References

- [1] X. Guo and K. Houser, "A review of colour rendering indices and their application to commercial light sources," *Light. Res. Technol.*, vol. 36, no. 3, pp. 183–197, Sep. 2004, doi: 10.1191/1365782804li112oa.
- [2] K. Houser, M. Mossman, K. Smet, and L. Whitehead, "Tutorial: Color Rendering and Its Applications in Lighting," *LEUKOS*, vol. 12, no. 1–2, pp. 7–26, Apr. 2016, doi: 10.1080/15502724.2014.989802.
- [3] D. Geisler-Moroder, "Color-rendering indices in global illumination methods," *J. Electron. Imaging*, vol. 18, no. 4, pp. 043015, 1–12, Oct. 2009, doi: 10.1117/1.3274623.
- [4] W. Davis, "Color quality scale," *Opt. Eng.*, vol. 49, no. 3, p. 033602, Mar. 2010, doi: 10.1117/1.3360335.
- [5] K. A. G. Smet, W. R. Ryckaert, M. R. Pointer, G. Deconinck, and P. Hanselaer, "Memory colours and colour quality evaluation of conventional and solid-state lamps," *Opt. Express*, vol. 18, no. 25, pp. 26229–26244, Dec. 2010, doi: 10.1364/OE.18.026229.
- [6] C. Li, M. Ronnier Luo, C. Li, and G. Cui, "The CRI-CAM02UCS colour rendering index," *Color Res. Appl.*, vol. 37, no. 3, pp. 160–167, Jun. 2012, doi: 10.1002/col.20682.
- [7] P. van der Burgt and J. van Kemenade, "About color rendition of light sources: The balance between simplicity and accuracy," *Color Res. Appl.*, vol. 35, no. 2, pp. 85–93, 2010, doi: 10.1002/col.20546.
- [8] A. David *et al.*, "Development of the IES method for evaluating the color rendition of light sources," *Opt. Express*, vol. 23, no. 12, pp. 15888–15906, Jun. 2015, doi: 10.1364/OE.23.015888.
- [9] M. S. Rea and J. P. Freyssinier, "Color rendering: Beyond pride and prejudice," *Color Res. Appl.*, vol. 35, no. 6, pp. 401–409, Dec. 2010, doi: 10.1002/col.20562.
- [10] A. David, K. A. G. Smet, and L. Whitehead, "Methods for Assessing Quantity and Quality of Illumination," *Annu. Rev. Vis. Sci.*, vol. 5, no. 1, pp. 479–502, Sep. 2019, doi: 10.1146/annurev-vision-091718-015018.
- [11] M. P. Royer, "IES TM-30-15 Is Approved—Now What?," *LEUKOS*, vol. 12, no. 1–2, pp. 3–5, Apr. 2016, doi: 10.1080/15502724.2015.1092752.
- [12] L. Neumann and J. Schanda, "Effect of interreflections in a room on the colour rendering of light source," in *Proceedings CGIV 2006*, 2006, pp. 283–286.
- [13] M. G. Bloj, D. Kersten, and A. C. Hurlbert, "Perception of three-dimensional shape influences colour perception through mutual illumination," *Nature*, vol. 402, no. 6764, pp. 877–879, Dec. 1999, doi: 10.1038/47245.
- [14] K. Doerschner, H. Boyaci, and L. T. Maloney, "Human observers compensate for secondary illumination originating in nearby chromatic surfaces," *J. Vis.*, vol. 4, no. 2, pp. 92–105, Feb. 2004, doi: 10.1167/4.2.3.
- [15] S. C. Pont, "Light: Toward a Transdisciplinary Science of Appearance and Atmosphere," *Annu. Rev. Vis. Sci.*, vol. 5, no. 1, pp. 7.1–7.25, Sep. 2019, doi: 10.1146/annurev-vision-091718-014934.
- [16] J. J. Koenderink, S. C. Pont, A. J. van Doorn, A. M. L. Kappers, and J. T. Todd, "The Visual Light Field," *Perception*, vol. 36, no. 11, pp. 1595–1610, Nov. 2007, doi: 10.1068/p5672.
- [17] E. Adelson and J. Bergen, "The Plenoptic Function and the Elements of Early Vision," in *Computational Models of Visual Processing*, M. Landy and J. Movshon, Eds. Cambridge, MA: The MIT Press, 1991, pp. 3–20.
- [18] C. Yu, E. Eisemann, and S. Pont, "Colour Variations Within Light Fields: Interreflections and Colour Effects," *Perception*, vol. 48, pp. 59–59, Sep. 2019, doi: 10.1177/0301006619863862.
- [19] A. A. Mury, S. C. Pont, and J. J. Koenderink, "Representing the light field in finite three-dimensional spaces from sparse discrete samples," *Appl. Opt.*, vol. 48, no. 3, pp. 450–457, Jan. 2009, doi: 10.1364/AO.48.000450.
- [20] C. Cuttle, "Research Note: A practical approach to cubic illuminance measurement," *Light. Res. Technol.*, vol. 46, no. 1, pp. 31–34, Feb. 2014, doi: 10.1177/1477153513498251.
- [21] T. Kartashova, D. Sekulovski, H. de Ridder, S. F. te Pas, and S. C. Pont, "The global structure of the visual light field and its relation to the physical light field," *J. Vis.*, vol. 16, no. 10, pp. 9, 1–16, Aug. 2016, doi: 10.1167/16.10.9.
- [22] L. Xia, S. Pont, and I. Heynderickx, "Light diffuseness metric, Part 2: Describing, measuring and visualising the light flow and diffuseness in three-dimensional spaces," *Light. Res. Technol.*, vol. 49, no. 4, pp. 428–445, Jun. 2017, doi: 10.1177/1477153516631392.